

Dynamics of CO Rebinding to Protoheme in Viscous Solutions

Taegon Lee, Jaehung Park, Jooyoung Kim, Sangwoo Joo,[†] and Manho Lim^{*}

Department of Chemistry and Chemistry Institute for Functional Materials, Pusan National University, Busan 609-735, Korea. *E-mail: mhl@pusan.ac.kr

[†]Department of Chemistry, Soongsil University, Seoul 156-743, Korea

Received November 17, 2008, Accepted November 30, 2008

We present the geminate rebinding kinetics measurements of CO to 2-methylimidazole (2-MeIm) bound ferrous protoporphyrin-IX (FePPIX) in alkaline glycerol/water mixtures at 293 K after photolysis. The kinetics was probed by monitoring the CO stretching mode using femtosecond vibrational spectroscopy. When 2-MeIm is used in excess, heme dimers that typically form in low viscosity solutions disappear as the viscosity of the solvent increases. Heme aggregates formed in low viscosity solutions turn monomeric as more 2-MeIm is added, suggesting that 6-coordinated heme, including a strong proximal histidine tends to be in the monomeric form. The vibrational band of CO in the 2-MeIm-FePPIX-CO is well described by a single Gaussian function centered at 1958 cm^{-1} and 28 cm^{-1} full width at half maximum. The efficiency and rate of the geminate rebinding of CO to the heme increase with viscosity of the solvent, suggesting that retention of the dissociated CO near the heme, for a longer period by the viscous solvent media, accelerates rebinding.

Key Words: CO Rebinding, Protoheme, Fs vibrational spectroscopy, Viscous solution

Introduction

Even the simplest of chemical reactions may become complex in biological systems as protein conformations can affect the rates, coordinates, and yields of the reaction throughout its course. For example, the rebinding of CO to myoglobin (Mb) is multiphasic and shows non-Arrhenius temperature dependence due to the inhomogeneity of protein conformation and conformational relaxation after deligation.¹ The rebinding of CO to Mb following photolysis of MbCO has long served as a model system for the investigation of how proteins can control reactions.² The enthalpic barrier of CO rebinding to Mb has been separated into proximal and distal contributions,³ with the proximal effect results due mainly to the Fe out-of-plane displacement^{3,4} and the distal effect arising from the spatial and orientational constraints imposed on CO by the distal pocket (the primary heme pocket).⁵ The proximal contribution was obtained by investigating the CO rebinding kinetics to bare heme both with and without the proximal ligand.³

Iron protoporphyrin-IX (FePPIX), also known as heme, is the prosthetic group of a large class of heme proteins. The bare heme has been used in investigating the intrinsic dynamics of CO rebinding to heme, free from protein structure and its conformational dynamics.⁶⁻¹¹ While FePPIX is an excellent model system for the active site of various heme proteins, the bare heme tends to dimerize and aggregate when exposed to solution, significantly perturbing the rebinding kinetics of CO to the heme.¹² Encapsulation of the heme compound in micelles was found to stabilize it in a monodispersed solution and thus prevents heme aggregation,^{13,14} however, the presence of the micelles also influence the rebinding kinetics. Previous studies found that low concentration heme can exist as a monomer in highly viscous alkaline solutions.^{9-11,15,16} However, there have been no systematic studies, as a function of solvent viscosity, on the heme aggregation and rebinding kinetics of CO to the heme.

The vibrational stretching mode of CO is very sensitive to its environment and is thus an excellent probe for the surroundings of CO as well as the CO bound molecule itself.¹⁷⁻²⁰ For example, the characteristics of the CO band (band position and bandwidth) changes dramatically with mutation of even 1 amino acid residue near the distal site in the Mb.²¹ Several CO stretching frequencies in MbCO have been observed and attributed to different conformers of the protein.¹⁷⁻²⁰

Here we have investigated aggregation of a CO bound bare heme with a proximal ligand in viscous solutions and found that, with highly excess 2-methylimidazole (2-MeIm), FePPIX-CO can exist as a monomer even in moderately concentrated glycerol solutions. We also characterized the vibrational spectrum of CO within monomeric 2-MeIm-FePPIX-CO in viscous solutions. A single Gaussian function well describes the CO band and confirmed the heme as a monomer in solutions of varying viscosities. Utilizing these sample conditions and femtosecond vibrational spectroscopy, we measured the geminate rebinding kinetics of CO to 2-MeIm-PPIX as a function of viscosity of the solvent and found that rebinding is controlled by diffusion of the dissociated CO.

Materials and Methods

Sample preparation. A 2.0 mM FePPIX stock solution was prepared by dissolving hemin (FePPIX chloride, Aldrich) in 1.0 M NaOD and then diluted into an appropriate deoxygenated glycerol/water mixture with 2-MeIm. The sample was reduced with an excess amount of freshly prepared sodium dithionite under N_2 . The reduced sample was bubbled with CO for approximately 10 min to form the 2-MeIm-FePPIX-CO. The final sample for the time-resolved spectroscopy was $[\text{FePPIX}] = 0.1 \text{ mM}$, $[2\text{-MeIm}] = 2 \text{ M}$, and $\text{pD} = 12$. The sample was loaded into a gas-tight 0.08-mm-pathlength flow cell with CaF_2 windows for kinetic measurements with the temper-

ature of the cell maintained at 293 ± 1 K. In contrast to 1-MeIm, the methyl group in the 2-MeIm is known to sterically inhibit formation of the *bis*-2-MeIm complex and preclude even excess amounts of the compound from competing with CO for the sixth ligation site to the Fe atom.⁸ Therefore, 2-MeIm is used as the axial ligand instead of 1-MeIm. In the absence of the added proximal ligand, solvent molecules can serve as proximal ligands,³ therefore, some of the heme can potentially form $\text{H}_2\text{O-FePPIX-CO}$ under our experimental conditions.

The femtosecond mid-IR spectrometer. The details of the fs mid-IR spectrometer have been described elsewhere.²² Briefly, 2 identical, homebuilt optical parametric amplifiers (OPA), pumped by a Ti:S amplifier, are used to generate a 575-nm pump pulse with 3.8 μJ of energy,²³ and a tunable mid-IR probe pulse.^{24,25} The visible pulse was generated by frequency doubling of signal pulse from one OPA and the mid-IR pulse by difference frequency mixing of signal and idler pulse of the other OPA. The isotropic absorption spectrum was measured by setting the polarization of the pump pulse at the magic angle (54.7) relative to the probe pulse. The broadband transmitted probe pulse was detected with a 64-element- $\text{N}_2(\text{I})$ -cooled HgCdTe array detector mounted on the focal plane of a 320 mm monochromator with a 150 l/mm grating, resulting in a spectral resolution of ca. 0.9 cm^{-1} /pixel at 1950 cm^{-1} . The pump-induced change in the absorbance of the sample $\Delta A = A_p - A_u$, was determined by chopping the pump pulse at half the repetition frequency of the laser and computing the difference between the pumped (A_p) and unpumped (A_u) absorbances. Due to the excellent short-term stability of the IR light source ($< 0.5\%$ rms), less than 1×10^{-4} rms in absorbance units after 0.4 s of signal averaging was routinely obtained. Time resolution of the instrument was < 180 fs full width at half maximum (FWHM).

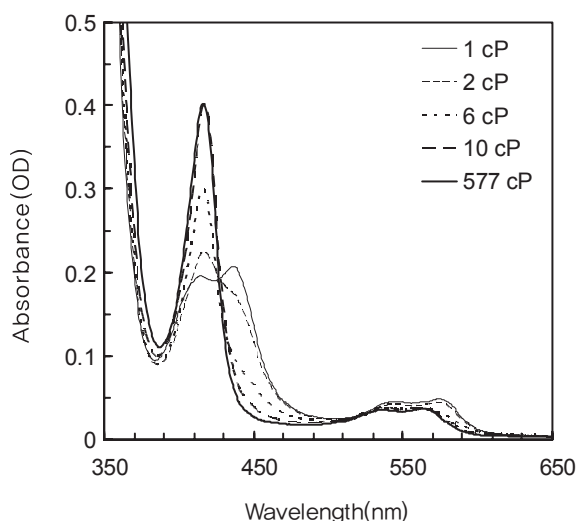
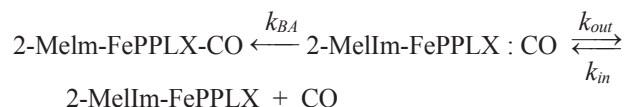


Figure 1. Equilibrium spectra of 0.1 mM 2-MeIm-FePPIX-CO with 0.5 M 2-MeIm in aqueous solution (1 cP) and glycerol/water mixtures (2 - 577 cP). Glycerol content in water was: 25% (2 cP); 45% (6 cP); 55% (10 cP); and 95% (577 cP) by volume.²⁸ Pathlength of the sample cell was 0.24 mm. The Soret band of the monomeric heme peaks at 418 nm and the band of aggregated heme peaks at 435 nm. Note that the peaks at 435 nm (418 nm) decrease (increase) as viscosity increase.

Kinetic model. A 3-state kinetic model²⁶ can be used to describe the rebinding process of CO to 2-MeIm-FePPIX after photolysis of 2-MeIm-FePPIX-CO



where the 2-MeIm-FePPIX:CO and 2-MeIm-FePPIX + CO represent a contact pair state²⁷ and the state of CO free in solution, respectively. The rate constants k_{BA} , k_{out} and k_{in} represent bond formation rate from the contact pair, escape rate of CO in contact to solvent, and contact formation rate from solvated CO, respectively. When $[2\text{-MeIm-FePPIX}] \ll [\text{CO}]$, this 3-state model can be simplified as⁸

$$\Delta A(t) = \Delta A_0 \left\{ I_g e^{-k_g t} + (1 - I_g) e^{-k_s t} \right\} = \Delta A_0 N(t) \quad (1)$$

where ΔA_0 is the absorbance change at $t = 0$ and $N(t)$ is the normalized population of the deligated heme at time t after photolysis. The quantity k_g and k_s are rate constants for the geminate and bimolecular phases of rebinding, respectively. The observed geminate rate (k_g) and geminate yield (I_g) are related to the intrinsic rates as follows: $k_g = k_{BA} + k_{out}$, $I_g = \{k_{BA} / (k_{BA} + k_{out})\}$.^{8,26}

Results and Discussion

Figure 1 shows equilibrium spectra of 0.1 mM FePPIX-CO with 0.5 M 2-MeIm in glycerol/water mixtures. While the Soret band in a highly viscous solution (95% glycerol in volume, 577 cP)²⁸ has one prominent band peaked at 418 nm, in low viscosity solutions (1 and 2 cP) there are two peaks at 418 and 438 nm. As the viscosity of the solution increases by increasing glycerol content, the bands at 438 nm (418 nm) decrease (increase) with an isosbestic point at 428 nm, suggesting that two species coexist in low viscosity solutions. FePPIX-

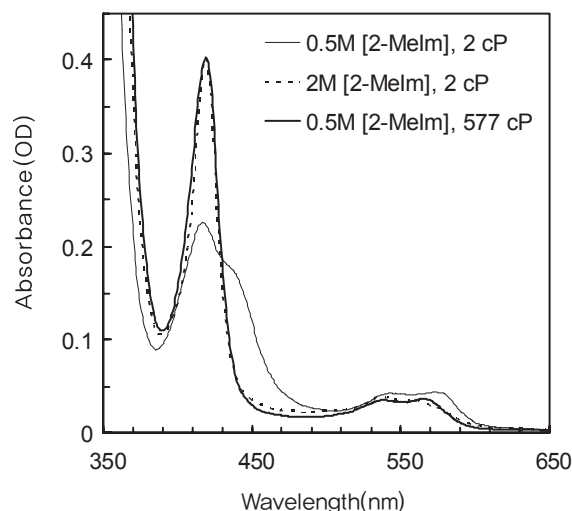


Figure 2. Equilibrium spectra of 0.1 mM 2-MeIm-FePPIX-CO with 0.5M (the thin solid line) and 2M (the dotted line) 2-MeIm in 25% glycerol (2 cP). The spectrum at 95% glycerol (577 cP) is shown to represent the spectrum of the monomeric heme.

CO tends to dimerize or aggregate when dissolved in aqueous alkaline solution,³ thus highly viscous alkaline solutions or micelles were used to prevent heme aggregation.^{9-11,15,16} The Raman spectrum of FePPIX-CO in a 2-MeIm solution, revealing the stretching mode of the Fe atom of the heme and N atom of the 2-MeIm, $\nu_{\text{Fe-N}}$ at 212 cm^{-1} , confirmed that 2-MeIm serves as a proximal ligand of the heme.³ The Soret band of a monomeric H₂O-FePPIX-CO is known to peak at 411 nm and the band at 418 nm is a characteristic of the monomeric 2-MeIm-FePPIX-CO compound.³ The Soret band at 438 nm likely arises from heme aggregates and is clearly indicative of the existence of heme aggregates in low viscosity solutions. The concentration of aggregates decreases as the viscosity of the solution increases. If all the coordination sites of the FePPIX are preoccupied (i.e., 6-coordinated by a proximal ligand and CO), it has a reduced tendency towards aggregation. In the absence of added proximal ligands such as 2-MeIm, solvent molecules can easily take on the role,³ and thus H₂O-FePPIX-CO can form. However, the weak bonding between the solvent molecule and the Fe atom²⁹⁻³¹ leads to 5-coordinated FePPIX-CO that tends to aggregate. Therefore, high viscosity solvent is required to prevent aggregation of FePPIX-CO with 0.5 M 2-MeIm. Evidently, all the monomeric FePPIX-CO bound the proximal ligand, 2-MeIm in our experimental conditions, producing 2-MeIm-FePPIX-CO. As shown in Fig. 2, a large fraction of FePPIX-CO forms aggregates in the 2 cP solution. However, when 2M 2-MeIm was used, the Soret band in the 2 cP solution sharpened dramatically (Fig. 2) and mimicked that of the monomeric 2-MeIm-FePPIX-CO obtained in the 577 cP solution, suggesting that the majority of the compound is coor-

minated by 2-MeIm (2-MeIm-FePPIX-CO) and is in a monomeric form even in the 2 cP solution. This observation suggests that the compound coordinated with 2-MeIm has less of a tendency to aggregate. Therefore, we employed 2 M 2-MeIm in investigating the rebinding kinetics of CO to monomeric 2-MeIm-FePPIX as a function of the viscosity of the solution (37-252 cP).²⁸ Fig. 3(a) shows the absorption spectra of 2-MeIm-FePPIX-CO with 2 M 2-MeIm in the viscosity range of 37-252 cP. All the absorption spectra can be overlapped with the Soret band peaking at 418 nm, confirming that 2-MeIm-FePPIX-CO is indeed in a monomeric form under these experimental conditions. Thus, any variation in the kinetic measurements of these samples results from inherent properties of the solvent, namely viscosity.

Fig 3(b) shows the vibrational band of the CO stretching mode of 2-MeIm-FePPIX-CO in viscous solutions that is well described by a Gaussian function centered at 1958 cm^{-1} with 28 cm^{-1} FWHM. It is similar to the CO band of H₂O-FePPIX-CO in an 80% glycerol (v/v) solution, showing a single band centered at 1955 cm^{-1} with $\sim 23\text{ cm}^{-1}$ FWHM.⁵ The position of the CO band is known to be sensitive to the nature of the proximal ligand.³² The position and FWHM of the observed vibrational band are independent of the solvent viscosity, corroborating that 2-MeIm-FePPIX-CO is indeed in a monomeric form in a modest to high viscosity solvent when 2 M 2-MeIm is used. Since the vibrational band of the CO in the heme aggregates would have different characteristics from that in the monomer, if there were heme aggregates in the sample, the observed vi-

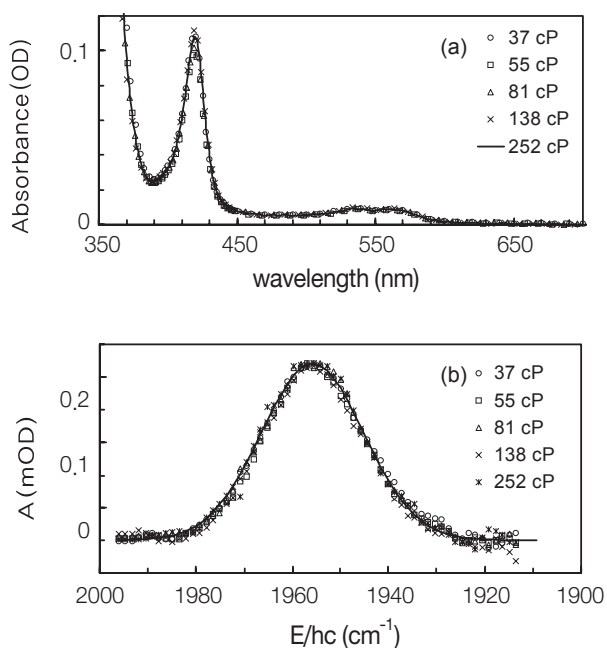


Figure 3. (a) Equilibrium electronic spectra of 0.1 mM 2-MeIm-FePPIX-CO used in a time-resolved study (pathlength of the sample cell = 0.08 mm). (b) The vibrational band of CO bound to 2-MeIm-FePPIX-CO in viscous solutions, well described by a single Gaussian centered at 1958 cm^{-1} with 28 cm^{-1} FWHM (the solid line). Data were obtained from time-resolved spectra at 0.3 ps pump-probe delay (symbols).

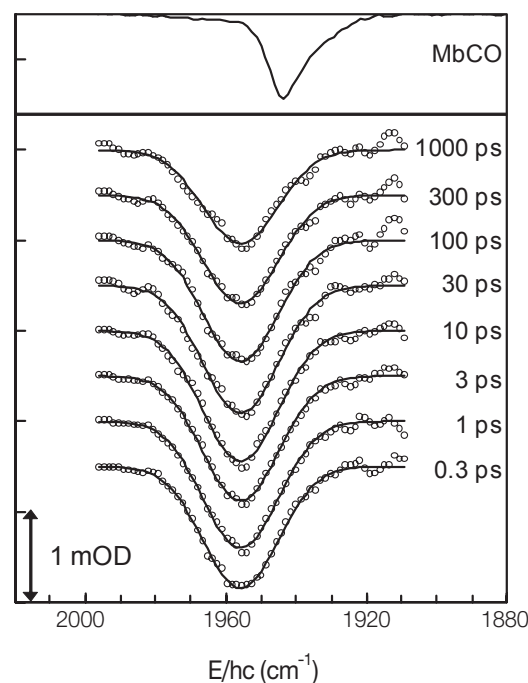


Figure 4. Representative time-resolved vibrational spectra of CO after photolysis of 2-MeIm-FePPIX-CO in 89.7% glycerol. Data (open circles) were fitted to single Gaussian plus linear function (the solid lines). Linear function models change in weak solvent absorption due to temperature changes induced by thermal relaxation of the excited heme. The signal from the solvent background was subtracted for clarity. Spectrum of MbCO is shown for comparison.

brational spectrum would possess several bands. A FWHM of 28 cm^{-1} is much broader than the observed $8\text{--}12\text{ cm}^{-1}$ in the CO band in carbonmonoxy myoglobin (MbCO),¹⁸ where the distal environments are well organized. Since CO in 2-MeIm-FePPIX-CO is exposed to inhomogeneous glycerol/water mixtures, broader FWHM can be attributed to the inhomogeneous distal environments.

Figure 4 shows the time-resolved vibrational spectra of bound CO after 575-nm photolysis of 2-MeIm-FePPIX-CO in an 89.7% glycerol (v/v) solution at 293K. Data were collected for pump-probe delay times longer than 0.3 ps to avoid contributions from the truncated free induction decay of bound CO and from coherent signals occurring when pump-probe pulses are overlapped.^{33,34} The negative-going features (bleach) arise from the loss of bound CO, the magnitude of which is proportional to the population of the 2-MeIm-FePPIX produced by the photolysis of CO from the 2-MeIm-FePPIX-CO. The bleach appears faster than the time-resolution of the instrument (0.18 ps). The ultrafast photodissociation of CO from heme was suggested from the observation of a deligated-heme-like Soret band absorption spectrum within 50 fs after photolysis of the heme proteins.³⁵ The ultrafast bleach of the vibrational band for the bound ligand was also observed in CO-bound as well as NO-bound heme proteins.^{22,36,37} The bleach spectrum is identical to the equilibrium spectrum of bound CO, with the exception that it appears as a negative signal. The decrease in the magnitude of the bleach results from the rebinding of CO to the parent molecule (geminate recombination). The efficiency and the rate of the geminate rebinding were characterized by fitting the normalized bleach signal as a function of time.

Figure 5 shows the survival fraction of the deligated 2-MeIm-FePPIX after photolysis of 2-MeIm-FePPIX-CO in 73–90% glycerol/water (v/v) solutions at 293 K. Glycerol content was carefully chosen to vary the viscosity of the solution within a broad range (37–252 cP).²⁸ The efficiency of CO geminate rebinding varies with the viscosity of the solvent as does the rate of rebinding, with both rebinding efficiency and rate increasing with viscosity of the solvent. When the range of the data is much shorter than $1/k_s$, equation (1) can be simplified to: $I_g e^{k_g t} + (1 - I_g)$. The rebinding kinetics was fitted to an exponential function plus constant, resulting in the geminate yield, $I_g = 13\text{--}21\%$, and the geminate rate, $k_g = 9\text{--}75 \times 10^8\text{ s}^{-1}$ (time constants of 1.1–0.13 ns). From these parameters, the intrinsic rates for the 3-state kinetic model were calculated. Table 1 summarizes the fitted parameters and the calculated intrinsic rates for the 3-state kinetic model. The rebinding rate from the contact pair, k_{BA} , increases with viscosity, ranging from 1.2 to $13 \times 10^8\text{ s}^{-1}$ (time constants of 8–0.8 ns) and is con-

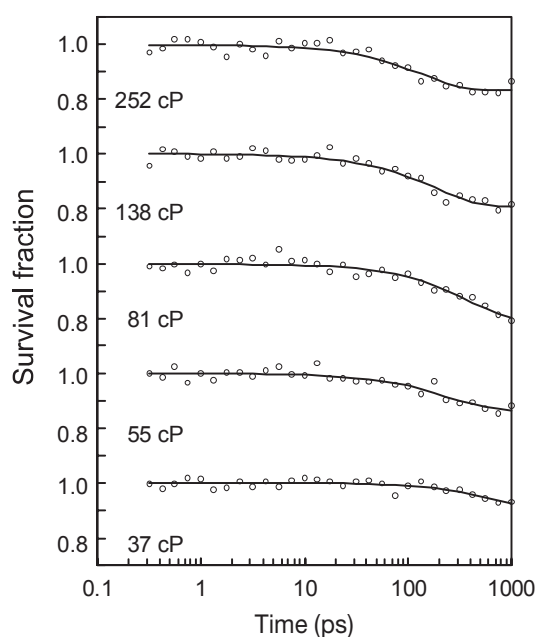


Figure 5. Survival fraction of the unbound 2-MeIm-FePPIX after photolysis of 2-MeIm-FePPIX-CO in viscous solutions at 293 K. The data (open circles) were fitted to a 3-state model (the solid lines) described in the text.

sistent with previous measurements using time-resolved optical spectroscopy in the Soret band.³ From the change in the Soret band of the sample in 80–95% glycerol (v/v) solutions, the reported geminate rate and yield was $8\text{--}47 \times 10^8\text{ s}^{-1}$ and 7–20%, resulting in $k_{BA} = 2\text{--}3 \times 10^8\text{ s}^{-1}$.³

The rebinding of CO to H₂O-FePPIX after photolysis of H₂O-FePPIX-CO is nonexponential with k_{BA} reported to be $1.5 \times 10^{10}\text{ s}^{-1}$ in 80% glycerol solution. The nonexponential rebinding is attributed to the distribution of the heme-doming geometries of the deligated heme. Exponential rebinding kinetics is expected if the rebinding is slower than the fluctuational averaging rate for heme-doming geometries. The averaging rate was estimated to be $3.3 \times 10^9\text{ s}^{-1}$ at 80% glycerol, a solvent relaxation rate at 290K,³⁸ value in good agreement with our observed exponential rebinding rate of $8\text{--}47 \times 10^8\text{ s}^{-1}$. While the rebinding rate of CO to 2-MeIm-FePPIX is more than 10 times slower than that of H₂O-FePPIX, it is more than 100 times faster than that to Mb after photolysis of MbCO. The rebinding rate of CO of Mb after photolysis of MbCO is exponential with $k_{BA} = 2.8 \times 10^6\text{ s}^{-1}$ in 75% glycerol. Much slower rebinding of CO to Mb has been attributed to the presence of the primary heme pocket in Mb.^{3,5}

The ratio of the rebinding rates of 2-MeIm-FePPIX and Mb was used to find the free energy difference in the rebinding bar-

Table 1. Fitted geminate parameters and calculated intrinsic rates for the 3-state kinetic model

Solvent	Glycerol % (v/v)	Viscosity ²⁸ (cP)	k_{BA} ($10^8/\text{s}$)	k_{out} ($10^8/\text{s}$)	k_g ($10^8/\text{s}$)	I_g
	73.3	37	1.2 ± 0.2	7.8 ± 0.5	8.9 ± 0.5	0.13 ± 0.01
	77.3	55	5.6 ± 0.9	35 ± 8	41 ± 9	0.14 ± 0.04
	80.9	81	5.5 ± 0.8	20 ± 7	26 ± 6	0.21 ± 0.04
	85.3	138	11 ± 1	46 ± 2	57 ± 3	0.19 ± 0.02
	89.7	252	13 ± 2	62 ± 1	75 ± 3	0.17 ± 0.05

rier due to the presence of the primary heme pocket and protein matrix.³ The difference in the free energy barrier, ΔG , was calculated to be 12 ± 1 kJ/mol at 293 K, using the equation:³

$$\exp\left(-\frac{\Delta G}{RT}\right) = \frac{k_{BA}(\text{Mb})}{k_{BA}(\text{2-MeIm-FePPIX})}$$

However, care has to be taken in the interpretation of this difference in the free energy barrier. Contribution from the protein matrix itself can be accessed from the rebinding kinetics of heme proteins without the primary heme pocket. The geminate rebinding of CO to carboxymethyl cytochrome *c* (Ccytc) in water, a heme protein without the primary heme pocket, was nonexponential and the average rate was found to be $7.4 \times 10^9 \text{ s}^{-1}$,³⁹ more than 3 orders of magnitude faster than that to Mb in water ($5.6 \times 10^6 \text{ s}^{-1}$),²⁶ and even faster than the 2-MeIm-FePPIX. Evidently, the presence of an organized protein matrix without a specific structure like the primary heme pocket accelerates the rebinding by efficiently holding the dissociated CO near the Fe atom for a longer period. Clearly, the difference in the free energy barrier mainly arises not from the presence of the protein matrix, but from the unique structure of the primary heme pocket. Therefore, the contribution of the primary heme pocket to the rebinding barrier can be recalculated using: $\exp\left(-\frac{\Delta G}{RT}\right) = \frac{k_{BA}(\text{Mb})}{k_{BA}(\text{Ccytc})} = \frac{5.6 \times 10^6}{7.4 \times 10^9}$, resulting in $\Delta G = 17 \pm 3$ kJ/mol at room temperature. The primary heme pocket indeed plays a significant role in hindering efficient geminate rebinding of CO in Mb.

As can be seen in Table 1, the geminate rebinding becomes faster and more efficient as the viscosity of the solvent increases. The dissociated CO starts to diffuse away from the Fe atom immediately after photolysis. Using Stock's relation:

$$D = \frac{k_B T}{6\pi\eta a}$$

the diffusion coefficient of CO in the viscous media at 293K was calculated to be $2.9 \times 10^{-7} \text{ cm}^2/\text{s}$ at $\eta = 37$ cP and $4.3 \times 10^{-8} \text{ cm}^2/\text{s}$ at $\eta = 252$ cP. Here, the van der Waals *b* coefficient for CO was used to deduce the hard sphere radius, *a* = 2 Å.¹¹ While the CO in 37 cP travels 1.3 Å in 100 ps and 4.1 Å in 1 ns, the CO in 252 cP travels only 0.5 Å in 100 ps and 1.6 Å in 1 ns. Note that the travel distance is from the nascent location reached in photolysis. Clearly, the CO in 252 cP remains near the Fe atom for a longer period, increasing the chance of geminate rebinding. Therefore, we conclude that the longer retention of the dissociated CO by the viscous media is responsible for the faster and more efficient geminate rebinding of CO to the heme. Since the organized protein matrix of Ccytc can serve as an excellent trap for the diffusing CO, our conclusion is consistent with the much faster and more efficient geminate rebinding of CO to Ccytc.

In conclusion, we have found that, in the presence of highly excess 2-MeIm, 2-MeIm-FePPIX-CO can exist in a monomeric form even in modestly viscous solvents. The vibrational stretching mode of CO in 2-MeIm-FePPIX-CO is well described by a single Gaussian centered at 1958 cm^{-1} with 28 cm^{-1} FWHM. It is much broader than that in Mb and slightly blue-shifted compared with that in H₂O-FePPIX-CO. While the band is sensitive to the nature of the proximal ligand, characteristics of the CO band are independent of the viscosity of the solvent in modest to high viscosities. Under our experimental conditions, the efficiency of the geminate rebinding of CO to

2-MeIm-FePPIX was 13-21%, with a rate faster than $1 \times 10^8 \text{ s}^{-1}$. Both efficiency and rate increase with viscosity of the solvent, suggesting that viscous media retard the diffusion of the dissociated CO and thus accelerates geminate rebinding.

Acknowledgments. This work was supported by the Korea Research Foundation Grant funded by the Korean Government (MOEHRD) (KRF-2007-314-C00146).

References

- Austin, R. H.; Beeson, K. W.; Eisenstein, L.; Frauenfelder, H.; Gunsalus, I. C. *Biochemistry* **1975**, *14*, 5355-5373.
- Springer, B. A.; Sligar, S. G.; Olson, J. S.; Phillips, G. N., Jr. *Chem. Rev.* **1994**, *94*, 699-714.
- Ye, X.; Yu, A.; Georgiev, G. Y.; Gruia, F.; Ionascu, D.; Cao, W.; Sage, J. T.; Champion, P. M. *J. Am. Chem. Soc.* **2005**, *127*, 5854-5861.
- Ye, X.; Ionascu, D.; Gruia, F.; Yu, A.; Benabbas, A.; Champion, P. M. *Proc. Natl. Acad. Sci. U. S. A.* **2007**, *104*, 14682-14687.
- Lim, M.; Jackson, T. A.; Anfinrud, P. A. *Nature Struct. Biol.* **1997**, *4*, 209-214.
- Traylor, T. G.; Magde, D.; Taube, D. J.; Jongeward, K. A.; Bandyopadhyay, D.; Luo, J.; Walda, K. N. *J. Am. Chem. Soc.* **1992**, *114*, 417-429.
- White, D. K.; Cannon, J. B.; Traylor, T. G. *J. Am. Chem. Soc.* **1979**, *101*, 2443-2454.
- Cao, W.; Ye, X.; Georgiev, G. Y.; Berezhna, S.; Sjodin, T.; Demidov, A. A.; Wang, W.; Sage, J. T.; Champion, P. M. *Biochemistry* **2004**, *43*, 7017-7027.
- Hasinoff, B. B. *Arch. Biochem. Biophys.* **1981**, *211*, 396-402.
- Hill, J. R.; Cote, M. J.; Dlott, D. D.; Kauffman, J. F.; McDonald, J. D.; Steinbach, P. J.; Berendzen, J. R.; Frauenfelder, H. *Springer Series Chemical Physics* **1986**, *46*, 433-435.
- Miers, J. B.; Postlewaite, J. C.; Zyung, T.; Chen, S.; Roemig, G. R.; Wen, X.; Dlott, D. D. *J. Chem. Phys.* **1990**, *93*, 8771-8776.
- White, W. I. In *The Porphyrins*; Dolphin, D., Ed.; Academic: New York, 1979.
- Medhi, O. K.; Mazumdar, S.; Mitra, S. *Inorg. Chem.* **1989**, *28*, 3243-3248.
- Simplicio, J.; Schwenzler, K. *Biochemistry* **1973**, *12*, 1923-1929.
- Beece, D.; Eisenstein, L.; Frauenfelder, H.; Good, D.; Marden, M. C.; Reinisch, L.; Reynolds, A. H.; Sorensen, L. B.; Yue, K. T. *Biochemistry* **1980**, *19*, 5147-5157.
- Moore, J. N.; Hansen, P. A.; Hochstrasser, R. M. *Proc. Natl. Acad. Sci. U.S.A.* **1988**, *85*, 5062-5066.
- Adachi, S.; Sunohara, N.; Ishimori, K.; Morishima, I. *J. Biol. Chem.* **1992**, *267*, 12614-12621.
- Ansari, A.; Berendzen, J.; Braunstein, D. K.; Cowen, B. R.; Frauenfelder, H.; Hong, M. K.; Iben, I. E. T.; Johnson, J. B.; Ormos, P.; Sauke, T. B.; Scholl, R.; Schulte, A.; Steinbach, P. J.; Vittitow, J.; Young, R. D. *Biophys. Chem.* **1987**, *26*, 337-355.
- Balasubramanian, S.; Lambright, D. G.; Boxer, S. G. *Proc. Natl. Acad. Sci. U.S.A.* **1993**, *90*, 4718-4722.
- Muller, J. D.; McMahon, B. H.; Chien, E. Y.; Sligar, S. G.; Nienhaus, G. U. *Biophys. J.* **1999**, *77*, 1036-1051.
- Li, T.; Quillin, M. L.; Phillips, G. N., Jr.; Olson, J. S. *Biochemistry* **1994**, *33*, 1433-1446.
- Kim, S.; Jin, G.; Lim, M. *J. Phys. Chem. B* **2004**, *108*, 20366-20375.
- Lim, M.; Wolford, M. F.; Hamm, P.; Hochstrasser, R. M. *Chem. Phys. Lett.* **1998**, *290*, 355-362.
- Hamm, P.; Kaindl, R. A.; Stenger, J. *Opt. Lett.* **2000**, *25*, 1798-1800.
- Hamm, P.; Lim, M.; Hochstrasser, R. M. *J. Phys. Chem. B* **1998**, *102*, 6123-6138.
- Henry, E. R.; Sommer, J. H.; Hofrichter, J.; Eaton, W. A. *J. Mol. Biol.* **1983**, *166*, 443-451.

27. Jongeward, K. A.; Magde, D.; Taube, D. J.; Marsters, J. C.; Traylor, T. G.; Sharma, V. S. *J. Am. Chem. Soc.* **1988**, *110*, 380-387.
 28. Lide, D. R. *CRC Handbook of Chemistry and Physics*, 76th ed.; CRC Press, Inc.: 1995.
 29. Brault, D.; Rougee, M. *Biochemistry* **1974**, *13*, 4598-4602.
 30. Brault, D.; Rougee, M. *Biochem. Biophys. Res. Commun.* **1974**, *57*, 654-659.
 31. Rougee, M.; Brault, D. *Biochemistry* **1975**, *14*, 4100-4106.
 32. Vogel, K. M.; Kozlowski, P. M.; Zgierski, M. Z.; Spiro, T. G. *J. Am. Chem. Soc.* **1999**, *121*, 9915-9921.
 33. Hamm, P. *Chem. Phys.* **1995**, *200*, 415-429.
 34. Wynne, K.; Hochstrasser, R. M. *Chem. Phys.* **1995**, *193*, 211-236.
 35. Petrich, J. W.; Poyart, C.; Martin, J. L. *Biochemistry* **1988**, *27*, 4049-4060.
 36. Anfinrud, P. A.; Han, C.; Hochstrasser, R. M. *Proc. Natl. Acad. Sci. U.S.A.* **1989**, *86*, 8387-8391.
 37. Lim, M.; Jackson, T.; Anfinrud, P. In *Practical Spectroscopy*; Marcel Dekker, Inc.: 2001; Vol. 26, pp 191-226.
 38. Kleinert, T.; Doster, W.; Leyser, H.; Petry, W.; Schwarz, V.; Settles, M. *Biochemistry* **1998**, *37*, 717-733.
 39. Kim, J.; Park, J.; Lee, T.; Lim, M. *J. Phys. Chem. B* (in press).
-